

VAMPIRE: Vessel Assessment and Measurement Platform for Images of the REtina

A Perez-Rovira, T MacGillivray, E Trucco, K S Chin, K Zutis,
C Lupascu, D Tegolo, A Giachetti, PJ Wilson, A Doney, and B Dhillon

Abstract—We present VAMPIRE, a software application for efficient, semi-automatic quantification of retinal vessel properties with large collections of fundus camera images. VAMPIRE is also an international collaborative project of four image processing groups and five clinical centres. The system provides automatic detection of retinal landmarks (optic disc, vasculature), and quantifies key parameters used frequently in investigative studies: vessel width, vessel branching coefficients, and tortuosity. The ultimate vision is to make VAMPIRE available as a public tool, to support quantification and analysis of large collections of fundus camera images.

I. INTRODUCTION

VAMPIRE is an easy-to-use tool allowing efficient quantification of features of the retinal vasculature with hundreds or thousands of images. Most processing is performed automatically before user intervention, which is kept at a minimum. The VAMPIRE interface provides easy-to-understand visual feedback of the features extracted and a set of tools that allows the user to easily identify, locate and correct wrong measurements. No experience of image processing algorithms is assumed.

Retinal microvascular abnormalities seen on fundal photography are associated with diabetes, hypertension, stroke and cognitive impairment [1], [2], [3]. Often, diagnostic focus is placed on structural features of the vasculature such as vessel width, branching angles, and vessel tortuosity [4], [5], [6]. Retinal blood vessels have similar size and physiology to cerebral small vessels and may act as a surrogate marker for them. Abnormalities are often subtle and may be missed by visual observation or conventional retinal image inspection. Taking manual measurements in retinal fundus images is also time-consuming and laborious, slowing down significantly the analysis of large numbers of images. Hence the need for software tools that can process large numbers of images in an objective, effective and efficient manner.

Some systems have appeared recently for semi-automatic assessment of retinal vessels. They include RISA, ROPtool, and ROPnet, designed within the context of retinopathy of

Perez Rovira, Trucco, Chin and Zutis are with the School of Computing, Univ of Dundee, UK e.trucco@dundee.ac.uk

MacGillivray is with the Clinical Research Imaging Centre, Univ of Edinburgh, UK T.J.MacGillivray@ed.ac.uk

Lupascu and Tegolo are with the Dept of Mathematics and Informatics, Univ of Palermo, Italy lupascu,tegolo@math.unipa.it

Giachetti is with the Dept of Computer Science, Univ of Verona, Italy andrea.giachetti@univr.it

Wilson and Doney are with Ninewells Hospital, NHS Tayside, UK pj.wilson@nhs.net, a.doney@cpse.dundee.ac.uk

Dhillon is with the Princess Alexandra Eye Pavilion, NHS Lothian, UK Bal.Dhillon@luht.scot.nhs.uk

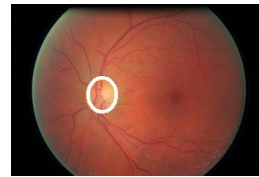
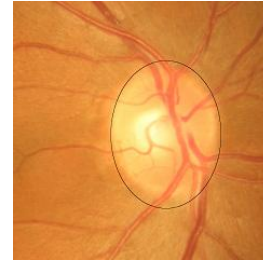


Fig. 1. Examples of OD location with ORIGA-light image (top; courtesy of Dr Liu Jiang, A-STAR Singapore) and Dundee diabetic screening image.

prematurity, and IDx, IVAN, CAIAR, SiVA and AVRnet in wider contexts. Space constraints preclude a comparative discussion. Apart from IDx, obtainable for research only, no system appears to be accessible publicly yet. 1 VAMPIRE starts with a segmentation of blood vessels and optic disc, followed by geometry estimation at vessel bifurcations, the tortuosity of major vessels, and fractal dimension of the vasculature. Most of the processing is hidden from the user, who is expected to provide only a minimal level of intervention after all measures are calculated. The current, beta version of VAMPIRE includes modules for vessel detection, branching angle measurements, vessel width estimation and tortuosity estimation. Optic disc location and fractal analysis are available and to be incorporated.

II. VAMPIRE OVERVIEW

A. User interface

VAMPIRE allows the user to load a set of images of arbitrary size. At the moment, no automatic quality assessment [7] is included. VAMPIRE locates the vasculature network and estimates branching coefficients, vessel widths, and tortuosity. The user can revise results efficiently, making corrections or discarding images. All measures, together with

metadata about the images, are saved by VAMPIRE in Excel files, ready for analysis.

To date, VAMPIRE has been run for tests and pilot correlational studies on images of resolution ranging from approximately 400×400 to 3000×3000 pixels, acquired by various commercial instruments. These include fundus cameras (e.g. Canon CR-DGi nonmydriatic at about 45° FOV), and a scanning laser ophthalmoscope (henceforth SLO), the OPTOS P200 ultra-wide-field-of-view. VAMPIRE was run also on the main public datasets or retinal images, DRIVE [8], STARE [9] and DIARETDB1 [10].

B. Landmark location

Purpose. To locate key retinal landmarks, namely the optic disc (OD), and the approximate path of the arcade vessels. This, in turn, enables location of the fovea, and the establishment of a retinal co-ordinates system.

Algorithm. Two steps are applied. First, a context-based search determines a point inside the OD with high confidence, leveraging anatomical constraints on the mutual location of OD and arcade vessels. Second, an elliptical shape model including an intensity model is fitted within a region centred on the point found to locate the OD contour [11].

Validation. The detection of the internal point has been validated with 230 images, including all the images in STARE, DRIVE and DIARETDB1 public datasets, plus 20 ultra-wide-field-of-view (200°) SLO images obtained with an OPTOS P200C SLO. Of these, 15 showed various lesions and 5 no lesion. Resolution was 3900×3092 pixels, cropped to a 700×605 region including macula and OD. OD location has been currently validated with two image sets: (a) *ORIGA-light*, courtesy of A-STAR Singapore, formed by $325\ 800 \times 800$ images cropped around the OD, which covers about 40% of the image area. Normal patients and glaucoma sufferers are included. On this set we achieve 100% correct location (defined as 90% or more of the estimated OD area overlapping the manually annotated one). (b) $286\ 2336 \times 3504$ images from the diabetes screening programme at Ninewells hospital, Dundee, including healthy and diseased retinas. On this set we achieve about 80% correct location, i.e., 240 correct results using the demanding definition from part (a) above. Most errors are due to very poor image quality (poor illumination or focus, OD obscured by severe lesions). Figure 1 show examples of images and locations from both datasets.

C. Vasculature detection

Purpose. To locate and represent the retinal vessel network.

Algorithm. We conducted trials with various vessel detection algorithms, including Soares et al. [12] and Lupascu et al. [13]. Currently, VAMPIRE implements a version of Soares's algorithm as the best compromise between speed and accuracy. In essence, the algorithm applies a multi-scale, 2-D Gabor wavelet transforms to emphasize the appearance of vessels, followed by supervised pixel classification with

a Bayesian classifier. Manually segmented images provide a labelled training set with two pixel classes, *vessel* and *non-vessel*. The authors report high accuracy (fraction of correctly classified pixels, 0.9466 and 0.9480 on DRIVE and STARE respectively). VAMPIRE implements this algorithm to generate a tree-like representation of the vasculature, as a pre-processing for measurements.

Validation. To complement the results reported in [12], we compared automatic segmentations with manual segmentations by human observers. Two authors, TMcG and APR, segmented manually a set of 20 fundus images. The segmentations of observer TMcG were taken as ground truth for the image database. The tracings of the second observer were taken as reference for computerized segmentation performance assessment, yielding an accuracy of 0.9591 against the first observer. The accuracy of the automatic segmentation against the first observer was 0.9570. Figure 2 shows three images, one from each public dataset, and the respective segmentations.

D. Vessel width

Purpose. To determine accurately the width of retinal vessels at specific locations.

Algorithm. Vessel width is computed in VAMPIRE as the length of the cross-section of the vessel mask taken perpendicularly to the vessel's estimated axis. The axis is obtained by thinning vessel regions to one-pixel-wide skeletons using Guos thinning algorithm [14].

Validation. We compared manual (2 observers) and automatic width estimates for 305 cross-sections of main and secondary vessels, both veins and arteries, from the 20-image set described in Section II-C. The set includes healthy and diseased (diabetic retinopathy) images. 176 cross-sections were taken within the first two retinal zones around the OD. For vessels within 2 OD diameters of the OD (zone 1 and 2), normally considered in AVR studies, the mean of the *absolute* differences between observers (4.9 pixels) was slightly higher than between VAMPIRE and each observer (3.1 and 4.0 pixels). The 95% confidence interval (CI) of the mean absolute differences between VAMPIRE and each observer (0.8 in both cases) was smaller than the 95% CI for the mean difference between the observers (0.98).

E. Vessel tortuosity

Purpose. To define and assess the degree of tortuosity of selected retinal vessels.

Algorithm. VAMPIRE implements a tortuosity measure integrating axis curvature and vessel width [15]. At the moment, only vessel segments between junctions are measured; estimates of the tortuosity of the whole vessel network are under study.

Validation. We compared tortuosity levels in the range *high*, *medium*, *absent* obtained by the program and established by a clinician, using 200 vessels spanning the three tortuosity classes. Performance compared favourably with that of four measures reported in the literature. We refer the reader to [15] for details.

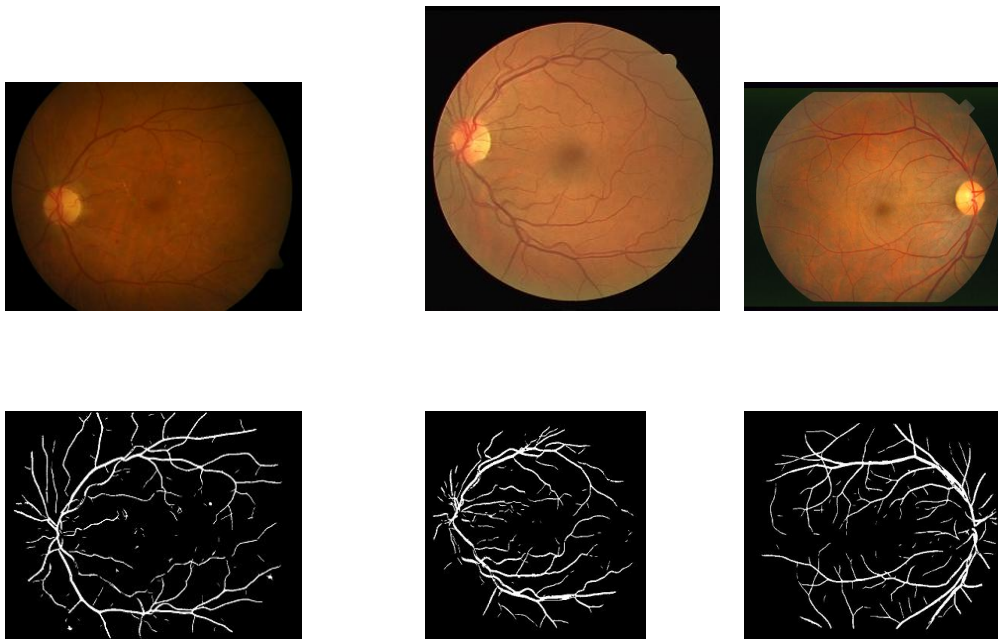


Fig. 2. Images and vascular segmentation from dataset DIARETDB1 (1500×1152), DRIVE (565×584), STARE (700×605).

F. Branching coefficients

Purpose. To quantify bifurcation geometry via branching angles and coefficients.

Algorithm. Vessel centerlines are created from the binary vessel map (Section II-C), and intersecting junction points of the three converging vessels are found for each junction. Junction locations are refined following [16]. Three best-fit straight lines, one per vessel, are used to find the optimal junction location. A second set of lines crossing the estimated location are now fitted to vessel points. Results are used to estimate junction angles. The bifurcation coefficient, b , is determined from the widths of parent, W , and that of the two child vessels, w_1, w_2 , as $b = \frac{w_1^2 + w_2^2}{W^2}$.

Validation. Approximately 5 venule and 5 arteriole branching points were measured in each of 20 images. Images were analyzed manually by two different raters using the angle measurement tool in ImageJ (<http://rsbweb.nih.gov/ij/>). Human and VAMPIRE measurements were then compared. The mean difference between the two human raters was 4.3° with 95% Confidence Interval (CI) of -13.9° to 22.4° ; the mean difference between human and computer was 5.8° with 95% CI of -17.5° to 29° , showing good algorithm accuracy.

Examples. Figure 3 shows two bifurcations with the respective branching coefficient and angles.

G. Fractal analysis

Purpose. To compute monofractal and multifractal measures of the human retinal vasculature.

Algorithm. The fractal dimension (FD) characterizes complex, repeating geometrical patterns at different spatial scales. In our case, FD measures the degree of branching complexity of the vasculature tree. FD changes have been associated, among others, with early diabetic retinopathy [17], which has

been found to yield a lower FD for the retinal vasculature than in control images. The cause for this discrepancy is not yet clear. Decreased FD has also been associated with ageing and hypertension

FD is generated by monofractal analysis, but the complexity of the vascular network is better captured by multifractal analysis (MFA), which resolve better local density variations. MFA is performed using the generalized sand-box method [18]. This selects a random set of pixels and counts the number of vessel pixels in square regions centred at the selected pixels and with increasing linear dimension.

Validation. We tested MFA on the DRIVE and STARE datasets, and on our own image set. In summary, our results showed that the 95% CI in FD was considerably smaller for MFA compared to the monofractal approach, i.e., less than $\pm 0.1\%$ compared to approximately $\pm 7\%$. Also, with reasonable image quality, the repeatability of fractal analysis performed on automatic vessel segmentations is close to that found when processing vessels traced manually by two human observers.

III. EXAMPLES OF APPLICATIONS

We mention here two examples of studies led by independent authors in which VAMPIRE software has been used.

Lothian Birth Cohort 1936. This longitudinal study [1] investigates the determinants of differences in cognitive ageing. Intelligence test data were collected on almost everyone born in Scotland in 1936 at age 11 in the Scottish Mental Survey of 1947. 1091 of these individuals were traced and re-tested. Study participants completed cognitive tests, gave details of their medical history and social background, completed psychosocial questionnaires, and underwent physical examination at age 70 and 73 years. Blood samples were collected for genetic analysis. Retinal photographs and

MR brain imaging were also collected and analysed using VAMPIRE software.



Fig. 3. Two bifurcations detected by VAMPIRE with visualization of branching coefficients and angles values.

Lacunar stroke. Lacunar stroke accounts for 25% of ischemic strokes, but the causes of abnormalities of cerebral small vessels remain unknown. Retinal blood vessels were investigated with VAMPIRE measurements as possible markers for such events as having similar size and physiology to cerebral vessels. 253 patients (129 lacunar stroke, 124 cortical stroke), mean age 68 years, were recruited. The results of this study [4] suggest that venular disease, a hitherto under-researched area, may play a role in the pathophysiology of lacunar stroke, and that retinal microvascular abnormalities can act as biomarkers for cerebral small vessel disease.

IV. CONCLUSIONS AND FUTURE WORK

VAMPIRE is a software tool for efficient semi-automatic assessment of the retinal vasculature in fundus camera images. VAMPIRE is also an international collaborative project, currently of four image processing groups and five clinical centres. The tool aims to assist users in the quantification of features of the retinal vasculature without requiring any training in image processing. VAMPIRE has already been used in several studies, which have also served as pilots to improve functionalities and interface. The ultimate vision is to make VAMPIRE available as a public tool.

We are currently extending the validation of VAMPIRE modules, gathering increasingly extensive collections of images, catalogued by different attributes (e.g., patient condition, imaging device) and annotated by multiple experts. We are also using VAMPIRE in further clinical, cognitive and genetics studies, and planning further modules to meet the resulting demands and feedback. Finally, we are developing novel techniques for training-free vessel detection and accurate vessel width estimation.

ACKNOWLEDGMENT

We thank Alex Doney and Graham Leese (Ninewells Hospital, Dundee, Diabetic Screening) for the TENOVUS images; Jimmy Liu (A-STAR Singapore) for the ORIGA-light images; Ian Deary, Alan Gow, Janie Corley, Ross Henderson, Catherine Murray, and Alison Pattie (Centre for Cognitive Ageing and Cognitive Epidemiology, Dept of Psychology, University of Edinburgh) for the LBC1936 fundus photographs. LBC1936 is supported by Help The Aged/Age Concern and a Sidney De Haan award as part of the Disconnected Mind project. The lacunar stroke study was

partially supported by the Scottish Funding Council through SINAPSE (www.sinapse.ac.uk).

REFERENCES

- [1] N. Patton, T. Aslam, T. J. MacGillivray, A. Pattie, I. J. Deary, and B. Dhillon, "Retinal vascular image analysis as a potential screening tool for cerebrovascular disease," *Journal of Anatomy*, vol. 206, pp. 318–348, 2005.
- [2] F. Doubal, P. Hokke, and J. Wardlaw, "Retinal microvascular abnormalities and stroke - a systematic review," *J. Neurol. Neurosurg. Psychiatry*, vol. 80, no. 2, pp. 158–165, 2009.
- [3] J. Ding, N. Patton, I. J. Deary, M. W. Strachan, F. G. Fowkes, R. J. Mitchell, and J. F. Price, "Retinal microvascular abnormalities and cognitive dysfunction: a systematic review," *Brit. J. Ophthalmol.*, vol. 92, no. 8, pp. 1017–1025, 2008.
- [4] F. N. Doubal, T. J. MacGillivray, P. E. Hokke, B. Dhillon, M. S. Dennis, and J. M. Wardlaw, "Differences in retinal vessels support a distinct vasculopathy causing lacunar stroke," *Neurology*, vol. 72, pp. 1773–1778, 2009.
- [5] N. Patton, T. M. Aslam, T. J. MacGillivray, I. J. Deary, B. Dhillon, R. H. Eikelboom, K. Yogesan, and I. J. Constable, "Retinal image analysis: concepts, applications and potential," *Prog. Retin. Eye Res.*, vol. 25, no. 1, pp. 99–127, 2006.
- [6] J. S. Wolffsohn, G. A. Napper, S.-M. Ho, A. Jaworski, and T. L. Pollard, "Improving the description of the retinal vasculature and patient history taking for monitoring systemic hypertension," *Ophthalmic and Physiological Optics*, vol. 21, no. 6, pp. 441–449, 2002.
- [7] A. D. Fleming, S. Philip, K. A. Goatman, J. A. Olson, and P. F. Sharp, "Automated assessment of diabetic retinal image quality based on clarity and field definition," *Investigative Ophthalmology and Visual Science*, vol. 47, no. 3, 2006.
- [8] J. Staal, M. D. Abramoff, M. Niemeijer, M. A. Viergever, and B. van Ginneken, "Ridge-based vessel segmentation in color images of the retina," *IEEE Trans on Medical Imaging*, vol. 23, no. 4, pp. 501–509, 2004.
- [9] A. Hoover and M. Goldbaum, "Locating the optic nerve in a retinal image using the fuzzy convergence of the blood vessels," *IEEE Trans on Medical Imaging*, vol. 22, no. 8, pp. 951–958, 2003.
- [10] T. Kauppi, V. Kalesnykiene, J. K. Kamarainen, L. Lensu, I. Sorri, A. Raninen, R. Voutilainen, J. Pietila, H. Kalviainen, and H. Uusitalo, "The DIARETDB1 diabetic retinopathy database and evaluation protocol," *Proc. Medical Image Understanding and Analysis (MIUA)*, pp. 61–65, 2007.
- [11] A. Perez-Rovira and E. Trucco, "Robust optic disc location via combination of weak detectors," *Journ. of Modern Optics*, vol. 57, no. 2, pp. 136–144, 2010.
- [12] J.V.B. Soares, J.J.G. Leandro, R.M. Cesar, H.F. Jelinek, and M.J. Cree, "Retinal vessel segmentation using the 2-D Gabor wavelet and supervised classification," *IEEE Trans on Medical Imaging*, vol. 25, no. 9, pp. 1214–1222, 2006.
- [13] D. Tegolo C. Lupascu and E. Trucco, "FABC: Retinal vessel segmentation using AdaBoost," *IEEE Trans. on Inf. Tech. in Biomedicine*, vol. 14, no. 5, pp. 1267–1274, 2010.
- [14] Zicheng Guo and Richard W Hall, "Parallel thinning with two-subiteration algorithms," *Communications of the ACM*, vol. 32, pp. 359–373, 1989.
- [15] E. Trucco, H. Azegrouz, and B. Dhillon, "Modeling the tortuosity of retinal vessels: does calibre play a role?," *IEEE Trans. on Biom. Engin.*, vol. 57, no. 9, pp. 2239–2247, 2010.
- [16] C. L. Tsai, C. V. Stewart, H. L. Tanenbaum, and B. Roysam, "Model-based method for improving the accuracy and repeatability of estimating vascular bifurcations and crossovers from retinal fundus images," *IEEE Trans. on Inf. Tech. in Biomedicine*, vol. 8, no. 2, pp. 122–130, 2004.
- [17] N. Cheung, K. C. Donaghue, G. Liew, S. L. Rogers, J. J. Wang, S. Lim, A. J. Jenkins, W. Hsu, M.L. Lee, and T. Y. Wong, "Quantitative assessment of early diabetic retinopathy using fractal analysis," *Diabetes Care*, vol. 32, pp. 106–110, 2009.
- [18] A. Avakian, R. E. Kalina, E. H. Sage, A. H. Rambhia, K. E. Elliott, E. L. Chuang, J. I. Clark, J. Hwang, and P. Parsons-Wingerter, "Fractal analysis of region-based vascular changes in the normal and non-proliferative diabetic retina," *Curr. Eye Res.*, vol. 24, no. 4, pp. 274–280, 2002.